Available online at www.sciencedirect.com
ScienceDirect
Physics Procedia 69 (2015) 271 – 274
Physics Procedia

10 World Conference on Neutron Radiography 5-10 October 2014

First attempts on energy-selective neutron imaging at IBR-2

E.V. Lukin*, D.P. Kozlenko, S.E. Kichanov, A.V. Rutkauskas, G.D. Bokuchava, B.N. Savenko

Frank Laboratory of Neutron Physics, Joint Institute for Nuclear Research, 141980, Dubna, Russia

Abstract

A new neutron imaging facility has been started at the IBR-2 high flux pulsed reactor. It is attractive not only for traditional neutron imaging applications but in particular also for the development of modern energy-selective techniques using a time-of-flight methods. A short overview of the first obtained results of the energy-selected experiments by means of time-of-flight methods realised on neutron radiography and tomography station on high-flux pulsed reactor IBR-2 are presented.

Keywords: neutron radiography; energy-selective; time-of-flight

1. Introduction

The neutron radiography and tomography methods are the powerful tool of non-destructive analysis, which demonstrates importance in industrial and scientific research [Anderson et al. (2009) and Domanus (1992)]. The powerful part of neutron radiography method is energy-selective neutron radiography, which have some interesting advantages. Here, we can varies radiography absorption contrast between some different materials due complex dependences of neutron attention coefficient from neutron wavelength [Lehmann et al. (2009) and Kockelmann et al. (2007)]. Therefore, the energy-neutron radiography provides additional information about structural features like as mosaicity, grain preferred orientation, internal stresses. It should note, that to compare with neutron stress measured diffraction methods, the energy-dispersive radiography allows to obtained structural information for the

* Corresponding author: Tel.: +7-49621-62047
E-mail address: lukin@jinr.ru

doi:10.1016/j.phpro.2015.07.038

whole of an investigated object in same time and point-to-point scanning procedure becomes unnecessary.

It is known, that a separation energy of neutrons for radiography experiments can be realized by means of different ways. On a steady neutron sources the double-crystal monochromator systems can be achieved [Treimer et al. (2006)]. In additional, the neutron wavelength dispersion are realized by means of a mechanical energy selector [G. Kühne et al (2005)]. The different rotation speed and mechanical selector constructions defines the required energy band. However, then we use a double-crystal monochromator system or mechanical selector the same intensity losses and achieved field-of-view in radiography experiments is restricted. Another way for neutron wavelength dispersion is time-of-flight methods, which successfully used on pulse neutron sources [Kockelmann et al. (2007)]. The one of advantages of this method to concerning radiography method is possibility to obtain imaging for selected different neutron energies simultaneously.

The IBR-2 high flux pulsed reactor is one of the most powerful pulsed neutron sources in the world with an average power of 2 MW but a great power per neutron pulse of 1850 MW [Dragunov et al. (2012)]. The periodic operation of the IBR-2 reactor regimes with 5 Hz frequency and pulse duration for thermal neutrons of 240 μs, which takes possibility to realization the neutron energy selection by means of time-of-flight method.

In presented work we reports about first results of neutron radiography experiments with neutron energy selection. These obtained results could be basis for energy-dispersive mode realization on new neutron radiography and tomography station at long pulse reactor IBR-2 or others pulsed neutron sources.

2. Experimental

The test energy dispersive neutron radiography experiments have been performed on the 14th beamline of the IBR-2 high flux pulsed reactor. A L/D ratio of experimental station is 200.

The new radiography and tomography facility is equipped by a scintillator based detector system (fig. 1a) constructed by conventional scheme (fig. 1b). A ^{6}LiF/ZnS scintillator of 0.2 mm thickness was used in this detector. The light is focused on the CCD chip by an optical lens Nikon, 50 mm, 1:1.4D, AF-Nikkor. The CCD camera made by “VIDEOSCAN” company was used for light detection. The CCD chip size is 36x24 mm^2 with total dimensions 4008x2672. The pixel size is 9x9 μm^2. In conventional high-resolution mode the camera frame rate is ~2.3 fps. For frame rate increasing up to ~6.5 fps we used 4x4 binning mode, where four neighboring pixels was summed in one active spot. The camera was synchronized with reactor pulses starts. The reactor neutron pulse was dispersed to tree neutron wavelength regions: from ~0.2 Å to ~2 Å, from ~2 Å to ~3.7 Å and from ~3.8 Å to 8 Å. The one wavelength region are corresponded to time-of-flight channel width of ~10 ms. We performed 100 neutron images for each wavelength region, afterwards imaging data were summed.

The IBR-2 reactor provides a time-dependent neutron beam in wavelength range from ~0.2 to 8 Å with maximum neutron wavelength at ~1.8 Å (Fig. 1c).

The imaging data are subtracted by the dark current image and are divided to the incident neutron beam by means of an ImageJ software [Schneider et al. (2012)].

3. Results

For test energy dispersive neutron imaging experiments we chooses several similar sticks with equivalent diameter of 15 mm made from different materials: aluminum, steel, lead, and copper (Fig. 2a).

The neutron images of such tested metal objects are shown for each selected energy region in fig. 2 (b-d). From imaging data an intensity profile plots perpendicular to sticks length axe have been built for each energy region (Fig. 3a).

The obtained profiles have been treated by a well-known function: $I/_{I_0} = \exp(-\alpha L)$ for the linear neutron attenuation coefficient α calculation. The thickness of a cylinder across the neutron beam direction is changes as $L = 2\sqrt{R^2 - (x - x_c)^2}$, where x_c – point of a cylinder center and R is the cylinder radius. The average coefficients α for each sticks materials were calculated for different neutron energy range and shown on fig 4 (a). On Fig. 4b the theoretical calculated patterns of the linear neutron attenuation coefficient for Al, Fe, Pb and Cu materials are presented. The theoretical data have been obtained by means of the NXSPlotter software [M. Boin (2012)].

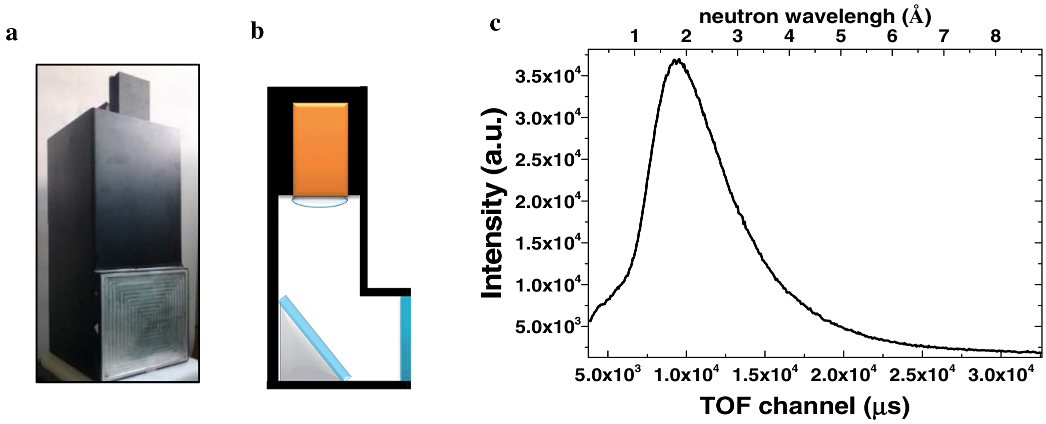

Fig.1. (a) The light-tight box of a scintillator-based detector on the radiography and tomography station at IBR-2 reactor. (b) The primitive schema of a scintillator-based detector. (c) The neutron spectra as function of time-of-flight channel and of neutron wavelength experimentally obtained on the new radiography and tomography station at the IBR-2 reactor.

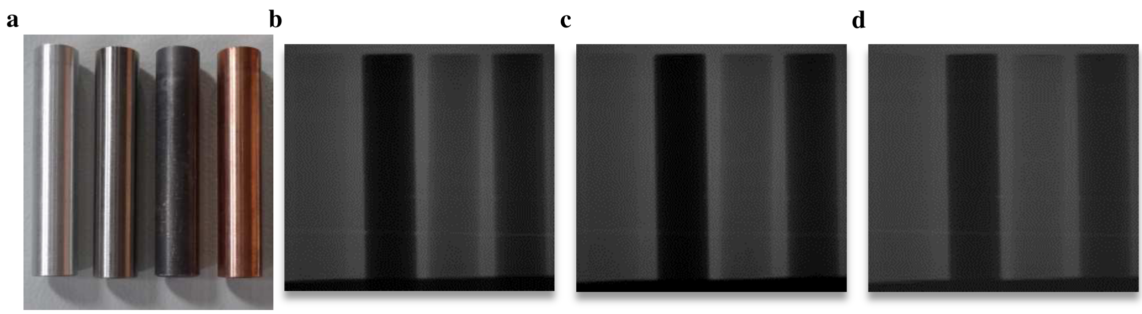

Fig. 2. (a) The photography of the cylinder materials (aluminum, steel, lead, copper). (b-d) The neutron images of the cylinder materials obtained for wavelength bands: (b) 0.2-2 Å, (c) 2-3.7Å, (d) 3.8-8Å

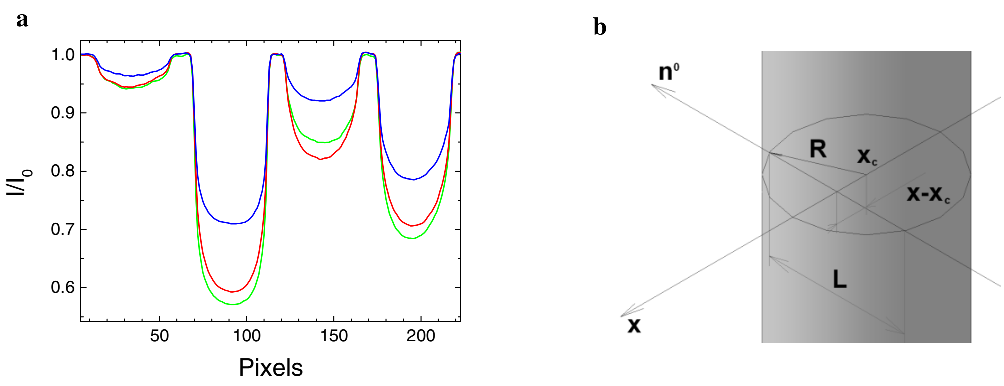

Fig. 3. (a) The plot profiles of the neutron images of four cylindrical sticks from different materials for different wavelength regions: red line - 0.2-2 Å, green one for 2-3.7 Å and blue - 3.8 - 8 Å. (b) The illustration of geometry of neutron beam direction through the cylindrical shape object, which used for attentuation coefficent. The notation are described in the text.

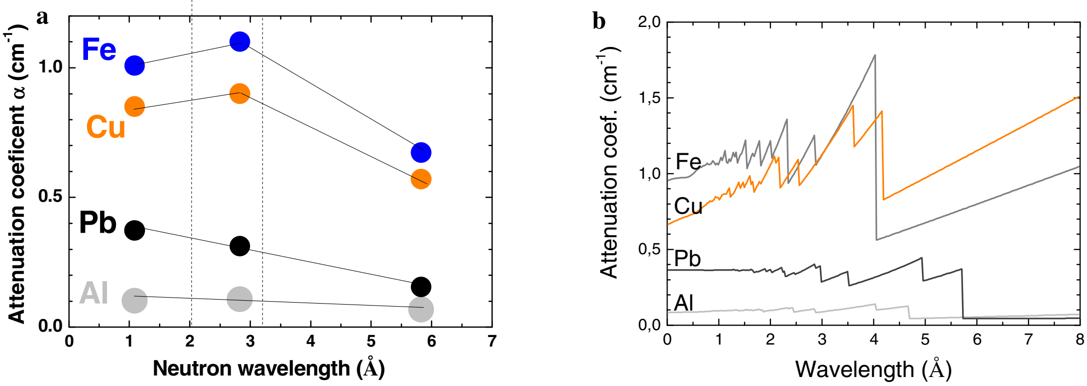

Fig. 4. (a) The calculated values of the linear neutron attenuation coefficient α for each wavelength interval. Dash lines represents the borders of a selected neutron wavelength region. (b) The theoretical dependence of the linear neutron attenuation coefficient as function of neutron wavelength.

In view of a great width of selected energy region in our experiments, the some tendency to resembling of obtained experimental data and corresponded theoretical curves are observed. It should note that all experimental data were obtained without imaging intensifier add-on. As final remarks, our first energy-dispersive radiography results shows good perspectives for realization neutron energy-selection mode with wide field-of-view via time-of-flight method on long pulse neutron source.

4. Conclusions

Recently, the neutron radiography and tomography facility have been developed at the IBR-2 high flux pulsed reactor. Now many activities directed on a development an energy-dispersive mode on this neutron radiography and tomography station. In our work, the results of a first attempt of energy selection via time-of-flight method in radiography experiments on pulsed reactor IBR-2 are reported.

Acknowledgements

This work has been supported by IAEA research contract #17217 and RFBR grant 14-22-01001-ofi_m.

References

Anderson, I.S., McGreevy, R.L., Bilheux, H.Z. (Eds.), 2009. Neutron Imaging and Applications: A Reference for the Imaging Community. Springer, New York, pp. 341.

Boin, M., 2012. nxs: a program library for neutron cross section calculations. Journal of Applied Crystallography 45, 603-607.

Domanus, J. C. (Ed.), 1992, Practical neutron radiography. Kluwer academic publishers, Netherlands, Dordrecht, pp. 269.

Dragunov, Yu. G., Tretiyakov, I. T., Lopatkin, A.V., et. al., 2012. Modernization of the IBR-2 pulsed research reactor. Atomic Energy 113, 29-38.

Lehmann, E.H., Frei, G., Vontobel, P., Josic, L., Kardjilov, N., Hilger, A., Kockelmann, W., Steuwer, A. 2009. The energy-selective option in neutron imaging. Nuclear Instruments and Methods in Physics Research A 603, 429–438.

Kockelmann, W., Frei, G., Lehmann, E.H., Vontobel, P., Santisteban, J.R., 2007. Energy-selective neutron transmission imaging at a pulsed source. Nuclear Instruments and Methods in Physics Research A 578, 421-434.

Kühne, G., Frei, G., Lehmann, E., Vontobel, P., Bollhalder, A., Filges, U., Schild, M. 2005. ICON – The New Facility for Cold Neutron Imaging at the Swiss Spallation Neutron Source SINQ. Swiss Neutron News, 28, 20-29

Schneider, C.A., Rasband, W.S., Eliceiri, K.W. 2012. NIH Image to ImageJ: 25 years of image analysis. Nature Methods 9, 671–675.

Treimer, W., Strobl, M., Kardjilov, N., Hilger, A., Manke, I., 2006. Wavelength tunable device for neutron radiography and tomography. Applied Physics Letters 89, 203504